Quantitative and Qualitative Intrapatient Comparison of ^{68}Ga-DOTATOC and ^{68}Ga-DOTATATE: Net Uptake Rate for Accurate Quantification

Irina Velikyan[1,2], Anders Sundin[2,3], Jens Sörensen[1,2], Mark Lubberink[1,4], Mattias Sandström[1,4], Ulrike Garske-Román[1], Hans Lundqvist[1], Dan Granberg[5], and Barbro Eriksson[5]

[1]PET and Nuclear Medicine, Department of Radiology, Oncology, and Radiation Science, Uppsala University, Uppsala, Sweden; [2]PET Centre, Centre for Medical Imaging, Uppsala University Hospital, Uppsala, Sweden; [3]Department of Radiology, Karolinska Institute and Karolinska University Hospital, Stockholm, Sweden; [4]Medical Physics, Uppsala University Hospital, Uppsala, Sweden; and [5]Department of Endocrine Oncology, Uppsala University Hospital, Uppsala, Sweden

Quantitative imaging and dosimetry are crucial for individualized treatment during peptide receptor radionuclide therapy (PRRT). ^{177}Lu-DOTATATE and ^{68}Ga-DOTATOC/^{68}Ga-DOTATATE are used, respectively, for PRRT and PET examinations targeting somatostatin receptors (SSTRs) in patients affected by neuroendocrine tumors. The aim of the study was to quantitatively and qualitatively compare the performance of ^{68}Ga-DOTATOC and ^{68}Ga-DOTATATE in the context of subsequent PRRT with ^{177}Lu-DOTATATE under standardized conditions in the same patient as well as to investigate the sufficiency of standardized uptake value (SUV) for estimation of SSTR expression. **Methods:** Ten patients with metastatic neuroendocrine tumors underwent one 45-min dynamic and 3 whole-body PET/CT examinations at 1, 2, and 3 h after injection with both tracers. The number of detected lesions, SUVs in lesions and normal tissue, total functional tumor volume, and SSTR volume (functional tumor volume multiplied by mean SUV) were investigated for each time point. Net uptake rate (K_i) was calculated according to the Patlak method for 3 tumors per patient. **Results:** There were no significant differences in lesion count, lesion SUV, K_i, functional tumor volume, or SSTR volume between ^{68}Ga-DOTATOC and ^{68}Ga-DOTATATE at any time point. The detection rate was similar, although with differences for single lesions in occasional patients. For healthy organs, marginally higher uptake of ^{68}Ga-DOTATATE was observed in kidneys, bone marrow, and liver at 1 h. ^{68}Ga-DOTATOC uptake was higher in mediastinal blood pool at the 1-h time point ($P = 0.018$). The tumor-to-liver ratio was marginally higher for ^{68}Ga-DOTATOC at the 3-h time point ($P = 0.037$). Blood clearance was fast and similar for both tracers. SUV did not correlate with K_i linearly and achieved saturation for a K_i of greater than 0.2 mL/cm^3/min, corresponding to an SUV of more than 25. **Conclusion:** ^{68}Ga-DOTATOC and ^{68}Ga-DOTATATE are suited equally well for staging and patient selection for PRRT with ^{177}Lu-DOTATATE. However, the slight difference in the healthy organ distribution and excretion may render ^{68}Ga-DOTATATE preferable. SUV did not correlate linearly with K_i and thus may not reflect the SSTR density accurately at its higher values, whereas K_i might be the outcome measure of choice for quantification of SSTR density and assessment of treatment outcome.

Key Words: ^{68}Ga; PET; [^{68}Ga]Ga-DOTA-TOC; [^{68}Ga]Ga-DOTA-TATE; neuroendocrine tumor; somatostatin

J Nucl Med 2014; 55:204–210
DOI: 10.2967/jnumed.113.126177

Combination of molecular imaging and internal radiotherapy targeted at receptors overexpressed in cancer cells is one example of advanced theranostics wherein the pretherapeutic imaging and radiotherapy are conducted with the same vector molecule, exchanging only the imaging and therapeutic radionuclides (*1*). This technique has become a powerful tool for the management of patients affected by neuroendocrine tumors (NETs) overexpressing somatostatin receptors (SSTRs). Approximately half of patients have metastatic disease at presentation, and early, accurate diagnosis and staging are crucial for therapy decisions. One of the main advantages of PET/CT is the possibility of quantifying tracer uptake and kinetics as a reflection of the processes underlying the disease and thus facilitating personalized diagnosis and therapy. PET/CT with ^{68}Ga-labeled somatostatin analogs is gradually becoming a new gold standard for NET imaging, replacing ^{111}In-DTPA-pentetreotide (Octreoscan; Mallinckrodt) scintigraphy. The method demonstrates specificity and sensitivity well above 90%, exceeding that of CT and scintigraphy (*2–4*). The superiority of ^{68}Ga-labeled somatostatin analogs in terms of specificity, sensitivity, staging accuracy, detection rate, quantification, and acquisition time over ^{18}F-FDG (*5*), ^{18}F-3,4-dihydroxyphenylalanine (*6*), ^{123}I-metaiodobenzylguanidine (*7,8*), ^{111}In-DTPA-pentetreotide (*9*), ^{18}F-NaF, and ^{99m}Tc-dicarboxypropanediphosphonate (*10*) has been demonstrated. The high impact of ^{68}Ga PET/CT on patient management can be illustrated by the fact that the course of treatments was changed or adjusted in 50%–60% of cases on the basis of ^{68}Ga PET/CT results (*11–15*). Thorough analysis of the publications on 16 clinical studies involving 567 patients with suspected thoracic or gastroenteropancreatic NETs suggested PET/CT with ^{68}Ga-labeled somatostatin analogs as an independent first-line diagnostic imaging method for this category of patients (*16*). ^{68}Ga-DOTATOC, ^{68}Ga-DOTATATE, and ^{68}Ga-DOTANOC have been extensively used in clinical studies demonstrating fast pharmacokinetics, target localization, blood clearance, and renal excretion as well as short scanning time, low radiation dose, high sensitivity, high resolu-

Received May 10, 2013; revision accepted Sep. 24, 2013.
For correspondence or reprints contact: Irina Velikyan, PET Center, Center for Medical Imaging, Uppsala University Hospital, SE-751 85 Uppsala, Sweden.
E-mail: irina.velikyan@bms.uu.se
Published online Dec. 30, 2013.

tion, high detection rate, high image contrast, and possibility for accurate quantification (*17*). Besides diagnosis, staging, prognosis, and therapy selection in NET disease, ^{68}Ga PET/CT has been applied in imaging of other SSTR-expressing tumors such as pheochromocytoma and paraganglioma, meningiomas, and melanoma, often having an effect on therapeutic management.

Individualized therapy planning with adjustment of injected radioactivity dose during peptide receptor radionuclide therapy (PRRT) of NETs is necessary because of high interpatient variability in healthy organ uptake (*18*). It has also been demonstrated that the tumor burden influences radiopharmaceutical distribution to healthy organs; in particular, higher tumor burden decreased accumulation of the radiopharmaceutical in the kidneys (*19*). PET/CT with ^{68}Ga-labeled somatostatin analogs may also become a valuable tool to determine the time point for the start of PRRT in relation to the termination of cold octreotide therapy in NET patients (*20*).

Refined and standardized protocols have been suggested because of the need for more accurate quantification, and their development is the focus of current research. High accuracy of the quantification is especially important for comparative studies of tracers and therapy monitoring when changes in tracer accumulation may be marginal and can be affected by several factors such as acquisition parameters and scanning protocols, examination time points, ongoing patient treatments, amount of the administered active substance, and radioactivity. The aim of the present work was to compare the performance of ^{68}Ga-DOTATOC and ^{68}Ga-DOTATATE (Fig. 1) in the same patient under uniform conditions and prolonged duration and to validate standardized uptake value (SUV) as a semiquantitative marker of SSTR expression in comparison with the net uptake rate (K_i) determined by tracer kinetic analysis.

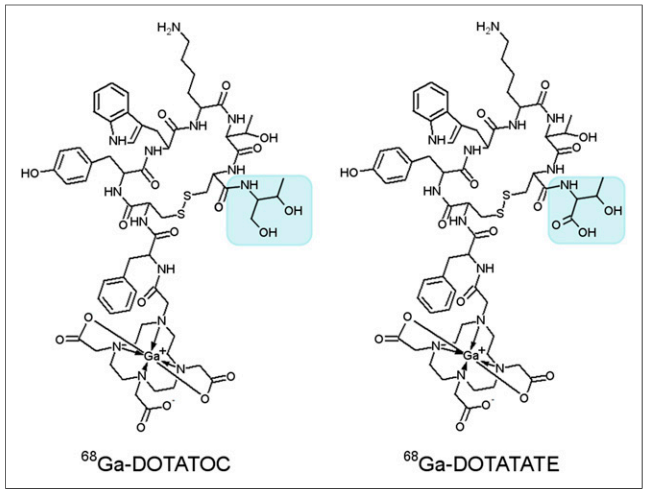

FIGURE 1. Structural formulas of ^{68}Ga-DOTATOC and ^{68}Ga-DOTATATE, where TOC and TATE stand, respectively, for D-Phe-Cys-Tyr-D-Trp-Lys-Thr-Cys-Thr(OH) and D-Phe-Cys-Tyr-D-Trp-Lys-Thr-Cys-Thr. Difference in structure is highlighted with blue square.

MATERIALS AND METHODS

Patients

Ten patients with metastatic gastroenteropancreatic NETs, confirmed by histopathology, underwent PET/CT examination after intravenous injection of ^{68}Ga-DOTATOC (24 ± 5 μg, 87 ± 16 MBq) or ^{68}Ga-DOTATATE (29 ± 5 μg, 92 ± 18 MBq) on 2 sequential days. The injected radioactivity was within the diagnostic reference level limits recommended by directive 97/43/EURATOM of the Council of the European Union (<200 MBq). The patients were divided into 2 groups of 5 to alter the sequence of administration of the agents.

Venous blood samples were collected at 5, 20, 45, 60, 120, and 180 min after injection for measurement of whole-blood and plasma radioactivity concentrations. Urine was sampled as voided, and total volumes and radioactivity concentrations were measured. Diuresis was not forced.

The study was approved by the Swedish Medicinal Products Agency (European Clinical Trials Database number 2011-001533-16) and the local ethical committee (diarienummer 2010/300). All patients gave signed informed consent.

Tracer Production and Quality Control

Good manufacturing practice–compliant production (*21*) of the tracers was accomplished within 1 h using a fractionation method (*22*) with subsequent product purification (*23*).

Data Acquisition

The patients fasted for 4 h before the examination, which was conducted on a Discovery ST16 PET/CT scanner (GE Healthcare) with a 15.7-cm axial and 70-cm transaxial field of view. After a low-dose CT scan for attenuation correction, a 45-min dynamic scan of the abdomen was started simultaneously with the administration of ^{68}Ga-DOTATOC or ^{68}Ga-DOTATATE. This scan was followed by 3 whole-body examinations from the eye level to the proximal thighs at 60, 120, and 180 min after injection (3-, 4-, and 5-min acquisition per bed position), each preceded by a low-dose CT scan. PET images were reconstructed with normalization and attenuation-weighted ordered-subset expectation maximization (2 iterations, 21 subsets) using the software supplied with the scanner, applying all appropriate corrections for dead time, randoms, scatter, coincidence, and detector normalization.

The last 25 min of the dynamic PET data were summed over time to create average images that were used to semiautomatically outline tumor volumes of interest over at most 3 lesions per patient at the 50% isocontour level using software developed at VU University Medical Centre, Amsterdam (*24*). Volumes of interest were then projected onto each frame to create tumor time–activity curves. An arterial volume of interest was defined by combining 2 × 2 pixel regions of interest in 10 consecutive image planes over the descending aorta in the image frame on which the first pass of the injected bolus was best seen. This volume of interest was projected onto each frame of the dynamic scan to obtain an arterial time–activity curve. Tumor volumes of interest were defined in a similar way on the 3 whole-body images. SUVs were calculated by normalized radioactivity concentrations to injected radioactivity per body weight. The total functional tumor volume was determined using 41% isocontour level volumes of interest. Evaluation of total SSTR volume (functional tumor volume multiplied by mean SUV [SUV_{mean}]) was performed on an Advantage Workstation 4.2 using VCAR (volume computer-assisted reading) software (GE Healthcare). SUV_{mean} in normal organs and tissues was determined by outlining circular regions of interest that were drawn at least 1 cm from the outer edges of organs.

Qualitative assessment of the examinations was performed in consensus by a nuclear medicine physician and a radiologist with 15–20 y of PET experience. The whole-body PET/CT examinations were evaluated for each patient by creating a visibility score for every lesion according to an arbitrary scale: 0, tumor not visualized but depicted at another time point or with the other tracer; 1, suspected tumor; and 2, definite tumor. The tumor-to-noise ratio in the examinations was also compared visually for both tracers at each time point.

K_i

Plasma input functions were obtained by multiplication of the arterial time–activity curve by the ratio of mean plasma to whole blood for

TABLE 1
Demographic and Clinical Characteristics of Patients

Patient no.	Months from diagnosis	Primary	Surgery	Tumor burden	K_i-67	Earlier treatment	Ongoing treatment	Body mass index	Hormones
1 (F, 67 y)	8	Pancreas	Ileocecal resection (ileus)	Pancreas, liver	3%	—	STZ + 5-FU, lanreotide,* SD	18.9 (50 kg)	CgA 62, Glu 214, Ins 171
2 (M, 53 y)	72	Lung, pancreas	Pancreas	Pancreas, lung, liver	11%	—	—	22.2 (70 kg)	—
3 (F, 73 y)	36	Pancreas	—	Pancreas, liver	31%	STZ + 5-FU	Octreotide acetate, long-acting*	26.1 (71 kg)	CgA 9.1
4 (M, 67 y)	72	Small intestine	Small-intestine resection	Liver, LN, paraaortal	<1%	—	IFN-α + octreotide acetate, long-acting,* SD	23.6 (79 kg)	CgA 20, U-5HIAA 31
5 (M, 58 y)	5	Small intestine	—	Primary liver, LN, mesentery, paraaortal	2%–3%	—	—	24.8 (75 kg)	CgA 1,640, U-5HIAA 2,457
6 (F, 63 y)	3	Small intestine	—	Primary liver, LN, abd, bone	<1%	—	—	22.3 (58.6 kg)	CgA 406, U-5HIAA 285
7 (M, 50 y)	2	Small intestine	Small intestine, LN, mesentery, omentum	Liver, LN, abd, mediastinum	12%–18%	—	Octreotide acetate, long-acting*	23.3 (85.1 kg)	CgA 8.2, U-5-HIAA 100
8 (M, 65 y)	48	Pancreas	—	Pancreas, liver	25%–30%	Carbo-VP 16, TMZ/Cap	TMZ + bevacizumab, SD	24.6 (71 kg)	CgA 20, PP 280
9 (F, 75 y)	22	Lung	Left pulmectomy	Liver		—	—	33 (80.5 kg)	CgA 7.2
10 (M, 44 y)	5	Small intestine	Small-intestine resection	Mesentary, peritoneum	10%	—	—	36 (120.5 kg)	CgA 6.0

*Stopped 4 wk before PET examination.

STZ = streptozotocin; 5-FU = 5-fluorouracil; SD = stable disease; CgA = chromogranin A (nmol/L); Glu = glucagon (ng/L); Ins = insulin (mE/L); LN = lymph node; IFN-α = interferon alpha; U-5HIAA = urinary 5-hydroxyindoleacetic acid (μmol/d); abd = abdomen; carbo = carboplatin; VP 16 = etoposide; TMZ = temozolomide; Cap = capecitabine; PP = pancreatic polypeptide (pmol/L).

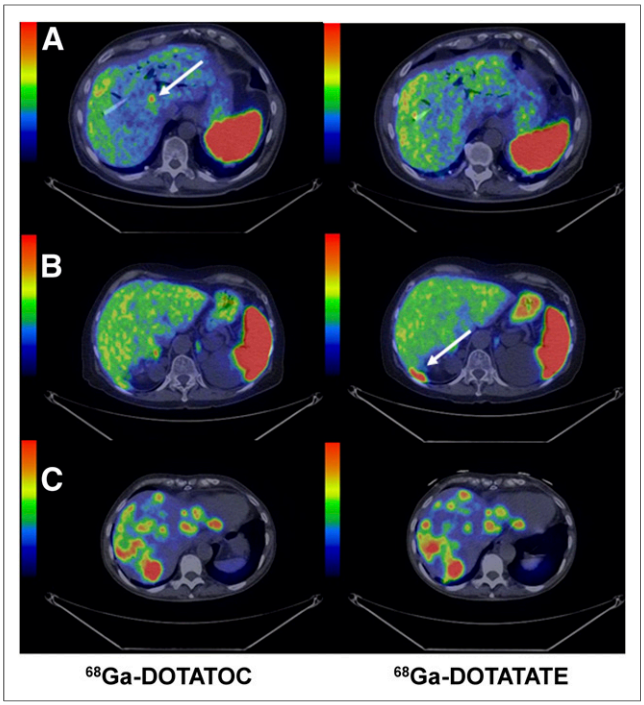

FIGURE 2. Transaxial images of liver demonstrating cases of higher detection rate for ^{68}Ga-DOTATOC (A: patient 6 [Table 1], PET/CT fusion); higher detection rate for ^{68}Ga-DOTATATE (B: patient 8 [Table 1], PET/CT fusion); and equal detection rate (C: patient 1 [Table 1], PET/CT fusion). Whole-body scans were conducted at 1 h after injection. Arrows point toward hepatic metastases.

the measured blood samples. The K_i of ^{68}Ga-DOTATOC and ^{68}Ga-DOTATATE was determined both using nonlinear regression of an irreversible 2-tissue-compartment model and using the Patlak method (*25*), which is a linearization of this model. K_i was calculated as the slope of the linear portion of the Patlak plot, starting 15 min after injection. The relations between K_i for both tracers and between SUV and K_i for each tracer separately were calculated by Deming regression.

Statistics

The statistical significance of differences and correlations between datasets were determined, respectively, by Wilcoxon matched-pairs test, Spearman correlation, and Deming regression ($P < 0.05$; GraphPad Prism software, version 5.00).

RESULTS

Patients

Demographics and clinical characteristics are given in Table 1. The median age of the patients was 64 y (range, 44–75 y), and the median duration from diagnosis was 15 mo (range, 2–72 mo). The patients did not have any clinical adverse reactions or side effects after the intravenous administration of either ^{68}Ga-DOTATOC or ^{68}Ga-DOTATATE.

Qualitative Evaluation of Lesions

One hundred one tumors were evaluated in 10 patients, and each patient had 10.1 ± 9.1 lesions (mean ± SD; range, 3–30). The readers evaluated 4 pancreatic tumors, 62 liver metastases, 11 mesenteric metastases, 5 peritoneal metastases, 15 retroperitoneal lymph node metastases, 3 mediastinal lymph node metastases, and 1 rib metastasis. The sum of visibility scores for the lesions at 1, 2, and 3 h were 100, 104, and 103, respectively, for ^{68}Ga-DOTATOC and 105, 107, and 101, respectively, for ^{68}Ga-DOTATATE. At 1 h, the score was higher for ^{68}Ga-DOTATOC in 2 patients, higher for ^{68}Ga-DOTATATE in 2 patients, and the same in 6 patients. The corresponding numbers were 3, 3, 4 and 3, 2, 5 at 2 and 3 h, respectively. The visibility score for all time points was higher for ^{68}Ga-DOTATOC in 4 patients, higher for ^{68}Ga-DOTATATE in 3 patients, and equal in 3 patients. The image quality in terms of tumor-to-noise ratio was visually rated as similar for both tracers in almost all patients and at all time points. Exceptions were patient 3, for whom ^{68}Ga-DOTATOC showed a better tumor-to-noise ratio at all 3 time points, and patients 4 and 6, for whom ^{68}Ga-DOTATATE showed a better tumor-to-noise ratio at 2 and 3 h, respectively.

In occasional patients, single liver metastases were clearly visualized with one tracer and not with the other (Fig. 2). Three liver metastases in patient 6 and 1 liver metastasis in each of patients 4 and 9 were clearly depicted by ^{68}Ga-DOTATATE but not by ^{68}Ga-DOTATOC. The reverse situation was found in patients 2 and 8, in whom 1 liver metastasis each was visualized with ^{68}Ga-DOTATOC but not with ^{68}Ga-DOTATATE. Only rarely were lesions visualized inconsistently between time points. In patient 7, 2 of the liver metastases were visualized with both tracers at 3 h but were not seen at 1 or 2 h. Similarly, a rib metastasis in the same patient was depicted by both tracers at 2 and 3 h but was missed at 1 h. In patient 10, a retroperitoneal lymph node metastasis with both tracers was missed at 1 h and showed up at 2 h but was then again not visible at 3 h.

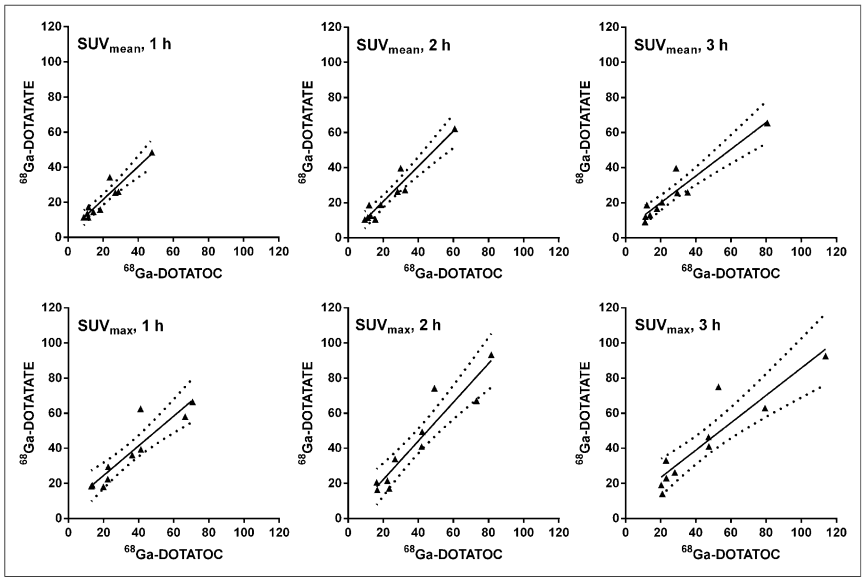

FIGURE 3. Correlation of tumor uptake (SUV_{max} and SUV_{mean}) of ^{68}Ga-DOTATATE and ^{68}Ga-DOTATOC, respectively, at 1-, 2-, and 3-h time points. Graphs show linear regression with 95% confidence band and r^2 values of 0.8891, 0.9204, and 0.8991, respectively, for SUV_{mean} and 0.8406, 0.8868, and 0.8443, respectively, for SUV_{max}.

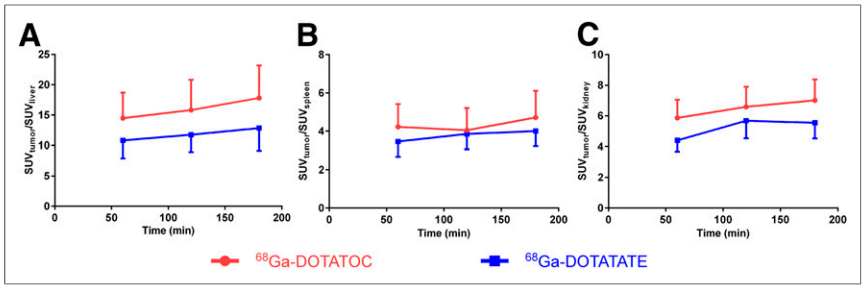

FIGURE 4. Ratio of tumor uptake (SUV_{max}) over liver (A), spleen (B), and kidney (C) uptake (SUV_{mean}) for ^{68}Ga-DOTATOC and ^{68}Ga-DOTATATE at whole-body PET/CT examinations 1, 2, and 3 h after tracer injection. Error bars indicate SEM.

The functional tumor volume and SSTR volume did not demonstrate any significant difference between the agents at any time point. Correlation of the uptake of ^{68}Ga-DOTATOC and ^{68}Ga-DOTATATE was significant, with corresponding Spearman r values of 0.89, 0.90, and 0.93 calculated for SUV_{mean} and 0.93, 0.93, and 0.93 calculated for maximum SUV (SUV_{max}) at 1, 2, and 3 h, respectively (Fig. 3).

Qualitative Evaluation of Normal Organs

There were marginal differences in tracer accumulation in normal organs. In particular, higher uptake of ^{68}Ga-DOTATATE was found in kidneys at 1, 2, and 3 h ($P = 0.002$, 0.020, and 0.004, respectively) and in liver at 1 and 2 h ($P = 0.037$ and 0.020, respectively). ^{68}Ga-DOTATOC uptake was higher in the mediastinal blood pool at 1 h ($P = 0.018$). No statistically significant difference was found in the vertebral body (bone marrow) at any time point.

Tumor–to–Normal-Organ Ratio

Tumor-to-liver ratio was similar for ^{68}Ga-DOTATOC and ^{68}Ga-DOTATATE at 1 and 2 h, whereas at the 3-h time point a marginally higher ratio was found for the former ($P = 0.037$) (Fig. 4A). For both tracers, this ratio was higher at 2 h than at 1 h ($P = 0.006$ and $P = 0.020$, respectively). Calculation of tumor-to-spleen ratios was based on 9 patients because patient 2 had undergone splenectomy. There was no statistically significant difference in tumor-to-spleen ratio between ^{68}Ga-DOTATOC and ^{68}Ga-DOTATATE at any time point, though for ^{68}Ga-DOTATOC the ratio was higher at 3 h than at 2 h ($P = 0.044$; Fig. 4B). The tumor-to-kidney ratio was higher for ^{68}Ga-DOTATOC than for ^{68}Ga-DOTATATE at 1 h ($P = 0.002$), 2 h ($P = 0.020$), and 3 h ($P = 0.004$) (Fig. 4C).

Tracer Kinetic Analysis

Time–activity curves of kidneys, liver, spleen, blood, and tumor for 195 min after injection are given in Figure 5. Blood clearance was fast and almost identical for both tracers. Radioactivity in the blood decreased to less than 5.3% and 4.7% of the peak level for ^{68}Ga-DOTATATE and ^{68}Ga-DOTATOC, respectively, within 45 min of the dynamic scanning and to 2.2% and 2.0% at 195 min after injection. The kinetics in kidney were similar in all patients. Higher variation was observed in the other organs and lesions. After 50 min, the accumulation in all organs plateaued. The tumor accumulation for each patient was represented by the lesion with the highest radioactivity uptake. ^{68}Ga-DOTATOC tumor uptake in all patients except one continually increased over time, whereas for ^{68}Ga-DOTATATE the uptake in 2 patients' tumors had decreased at 2 h and then again had increased at the 3-h examination. For 1 patient, the tumor uptake of ^{68}Ga-DOTATATE increased from 1 to 2 h and then decreased at the 3-h examination. No statistically significant difference was found in the tumor uptake of ^{68}Ga-DOTATOC and ^{68}Ga-DOTATATE at any time point (Fig. 6). For ^{68}Ga-DOTATOC, the tumor SUV_{max} and SUV_{mean} were higher at 2 h than at 1 h ($P = 0.002$ and 0.002), higher at 3 h than at 1 h ($P = 0.002$ and 0.002), and higher at 3 h than at 2 h ($P = 0.014$ and 0.018). The tumor SUV_{max} for ^{68}Ga-DOTATATE was higher at 3 h than at 1 h ($P = 0.020$), but there was no statistically significant difference in SUV_{mean} at any time point. After each PET examination, the patients were asked to void the bladder, and urine was collected. During the first 4 h after injection, 15.6% (SD, 9.2) of ^{68}Ga-DOTATOC and 11.9% (SD 4.1) of ^{68}Ga-DOTATATE was excreted into the urine.

K_i

K_i based on Patlak analysis correlated well with K_i based on compartment modeling for both tracers (Spearman $r = 0.89$ and 0.95 for ^{68}Ga-DOTATOC and ^{68}Ga-DOTATATE, respectively). K_i values based on Patlak analysis, which is the simpler of the methods, were used in the remainder of this work. The relation between SUV and K_i was not linear; instead, SUVs no longer increased for K_i values larger than 0.2 mL/cm^3/min (Figs. 7A and 7B). However, there was a good correlation between the K_i values for ^{68}Ga-DOTATOC and ^{68}Ga-DOTATATE (Fig. 7C). The use of SUV normalized for lean body mass instead of body weight did not alter this relationship.

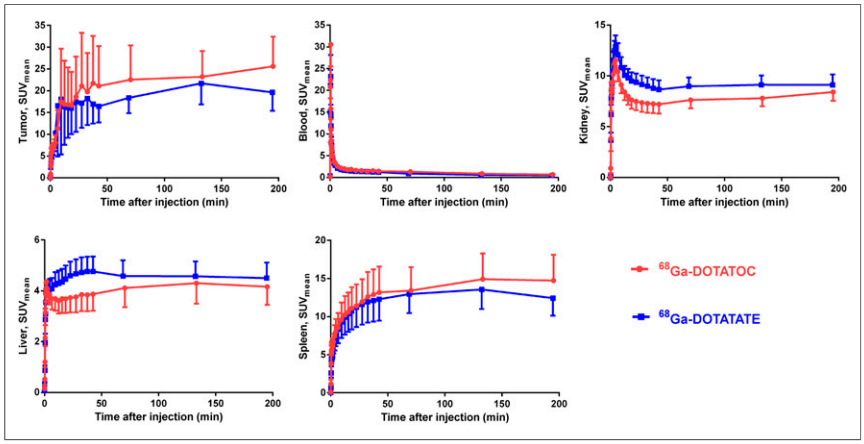

FIGURE 5. Accumulation of ^{68}Ga-DOTATOC and ^{68}Ga-DOTATATE in tumor and healthy organs (kidney, liver, and spleen), as well as blood clearance as function of time. SUV_{mean} is mean of all patients. Data are mean ± SEM.

DISCUSSION

Intrapatient evaluation and comparison of the performance of ^{68}Ga-DOTATOC and ^{68}Ga-DOTATATE was done under standardized conditions with the aim of assessing the preference of one or the other for imaging and patient selection in the context of PRRT with ^{177}Lu-DOTATATE. Quantitative and qualitative analyses of uptake kinetics, detection rate, image

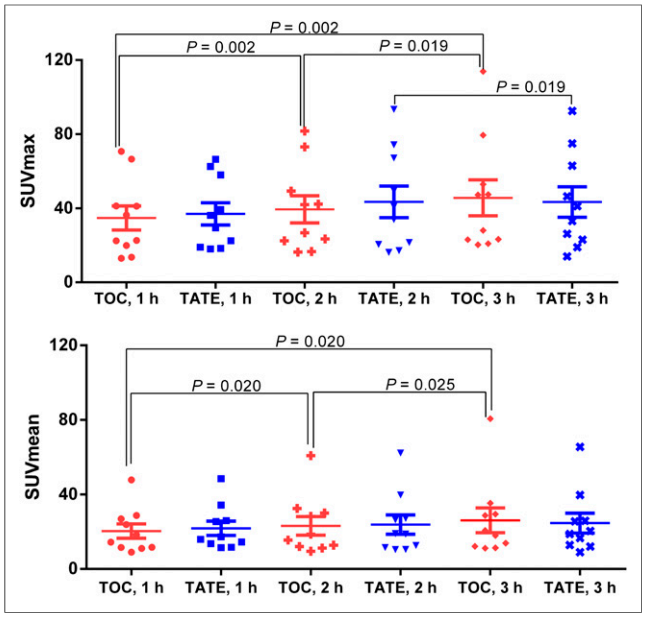

FIGURE 6. Tumor uptake (SUV_{mean} and SUV_{max}) at whole-body PET/CT examination with ^{68}Ga-DOTATOC (TOC) and ^{68}Ga-DOTATATE (TATE) 1, 2, and 3 h after tracer injection presented as mean with SEM. Each patient is represented by tumor with highest tracer uptake.

contrast, noise, and tumor and normal-tissue accumulation were performed.

The influence of peptide sequence, size and number of peptide rings, pharmacokinetic modifiers, chelator moiety, and radiometal type on the biologic properties of somatostatin analogs has been demonstrated by basic research (*15*). Hence, a 10-fold higher affinity for SSTR subtype 2 has been demonstrated for ^{68}Ga-DOTATATE than for ^{68}Ga-DOTATOC in vitro in transfected cell cultures (*26*). Nevertheless, no statistically significant difference in the uptake of ^{68}Ga-DOTATOC and ^{68}Ga-DOTATATE in SSTR-expressing monkey brain tissue sections in vitro or in rat organs such as adrenal, pancreas, and pituitary gland in vivo could be observed (*23*). Moreover, a clinical study involving 40 patients did not verify the 10-fold higher affinity for SSTR subtype 2 of ^{68}Ga-DOTATATE; on the contrary, SUV_{max} of ^{68}Ga-DOTATOC tended to be higher (*27*). The variation of the preference of one peptide analog over the other can be seen in clinical investigations using ^{111}In (*28*) and ^{177}Lu (*29*). In one study, ^{111}In-DOTATOC and ^{111}In-DOTATATE were used as surrogate agents for ^{90}Y and ^{177}Lu-comprising analogs (*28*). The authors justified the preferableness of the DOTATOC-based agent for radiotherapy with ^{90}Y. In contrast, a direct comparison of ^{177}Lu-DOTATOC and ^{177}Lu-DOTATATE favored the latter (*29*). Furthermore, a potential advantage was found for ^{68}Ga-DOTATOC over ^{68}Ga-DOTATATE in terms of detection rate and uptake degree (*27*). One plausible explanation for such a variation could be that even though SSTR subtypes 1 and 5 are the two most commonly expressed in NETs (*26*), the extensive difference in the subtype profile and population may diminish the alteration in apparent uptake. In our study, there was no unambiguous advantage of one agent over the other in terms of detection rate. The lesion visibility score for all time points was similar, although occasional lesions were better depicted with ^{68}Ga-DOTATOC than with ^{68}Ga-DOTATATE and vice versa. Quantitative differences in the normal-tissue uptake of either tracer were small. These differences might still be explained by the preferential binding to certain receptor subtypes with variable physiologic expression and did not affect the qualitative assessment of tumor visibility. ^{68}Ga-DOTATOC had slightly higher uptake in the mediastinal blood pool than did ^{68}Ga-DOTATATE, whereas blood radioactivity measured in the well-counter was not different. The reason is unclear but may be related to a slightly higher binding of ^{68}Ga-DOTATOC to endothelial surfaces.

Another possible reason for such variation in historical comparison could be the nonstandardized examination conditions, with variability in the administered dose of the peptide, scan duration, and interval between the examinations, as well as occasional use of contrast enhancement in PET/CT scans. In our study, we provided strictly standardized conditions such as a uniform time between the examinations with ^{68}Ga-DOTATOC and ^{68}Ga-DOTATATE, a uniform amount of injected radioactivity and peptide, and an identical scanning protocol for dynamic and static acquisitions for a prolonged period of 3.25 h. The amount of administered peptide in the present work was in the range (20–50 μg) of what was previously shown to result in higher tumor uptake and lower normal-organ accumulation (*30*). Varying tumor load expressing SSTRs of different concentrations acts as a sink, or compartment, and decreases the exposure of normal organs to the agent. The phenomenon has been observed for liver and spleen using ^{68}Ga-DOTATOC (*30*) and for kidneys using ^{68}Ga-DOTATATE (*19*). In addition, in our study, tumor accumulation after 1 h after injection did not increase for ^{68}Ga-DOTATATE but increased marginally for ^{68}Ga-DOTATOC. For clinical routine, diagnostic imaging at 1 h after injection might therefore be the optimal time point.

PET/CT generally uses semiquantitative SUV (*31–33*) as a measurement for patient selection, staging, and prognostic considerations. However, the above-mentioned discrepancies indicate that more accurate quantification methods are required for estimation of lesser differences expected during follow-up of therapeutic outcome, discrimination of pathologic from physiologic uptake, and inter- and intrapatient comparison of the various imaging agents. Tumor-to-spleen SUV ratio was found to be more accurate than SUV_{max} in the quantification of the response to PRRT by ^{68}Ga-DOTATOC PET/CT (*32*). However, our results showed that the variation in tumor-to-spleen SUV was determined by the increasing tumor accumulation whereas spleen uptake remained virtually constant during the course of the examinations. Tracer kinetic parameters, rather than SUV, might reflect the receptor density more accurately by contributing the additional dimensions of time and accumulation rate. Binding of the

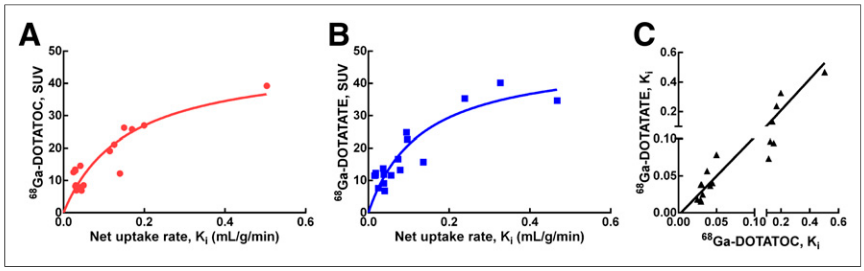

FIGURE 7. SUV is presented as function of K_i in tumors for ^{68}Ga-DOTATOC (A) and ^{68}Ga-DOTATATE (B). Solid lines are hyperbolic fits and are for visualization purposes only. Correlation is shown between K_i at 1 h after injection for ^{68}Ga-DOTATOC and ^{68}Ga-DOTATATE (C). Solid line is Deming regression with slope 1.06 and intercept 0.0. Axes are split to clarify relationship at low K_i values.

agents to the SSTRs can be considered irreversible since the radioactivity is trapped inside the cells. Thus, the steady-state K_i may better reflect the receptor concentration. The absence of linear correlation between SUV and K_i (Figs. 7A and 7B) indicates that SUV does not reflect receptor density correctly for tumors with high receptor expression and may lead to underestimation of the receptor expression. The reason for this phenomenon is probably that the availability of the peptide in plasma is the limiting factor for uptake of tracer in patients who have a large tumor burden with high SSTR expression. Another explanation could be that the plateau value corresponds to receptor saturation before receptor recycling to the cell surface. Our finding might at least partly explain why ^{68}Ga-DOTATOC PET/CT monitoring of PRRT response using changes in tumor SUV between baseline and follow-up was not trivial and did not correlate to the therapy outcome (*34*). The use of K_i might provide a more accurate measurement tool for evaluation of therapy response. Further systematic investigation is warranted in larger patient cohorts to explore the full potential and to prove the practical value of the methodology for patient care.

CONCLUSION

No statistically significant difference could be found in tumor uptake of ^{68}Ga-DOTATOC and ^{68}Ga-DOTATATE in terms of either SUV or K_i. Thus, both tracers can be used equally well for staging and patient selection for PRRT in NETs with ^{177}Lu-DOTATATE. However, the slight difference in healthy-organ distribution and excretion may render ^{68}Ga-DOTATATE preferable for PRRT planning. SUV did not correlate linearly with K_i and thus does not seem to reflect SSTR density accurately at higher values, suggesting that K_i is the outcome measure of choice for quantification of SSTR density and assessment of treatment outcome.

DISCLOSURE

The costs of publication of this article were defrayed in part by the payment of page charges. Therefore, and solely to indicate this fact, this article is hereby marked "advertisement" in accordance with 18 USC section 1734. This research was financially supported by the Swedish Cancer Society and a research grant from Uppsala University Hospital (ALF financial support). No other potential conflict of interest relevant to this article was reported.

ACKNOWLEDGMENTS

We greatly appreciate the technical assistance of Mimmi Lidholm, Annie Bjurebäck, Maj Wiberg, Lars Lindsjö, and Marie Ahlman in performing the scans and handling patients.

REFERENCES

1. Baum RP, Kulkarni HR. Theranostics: from molecular imaging using Ga-68 labeled tracers and PET/CT to personalized radionuclide therapy—the Bad Berka experience. *Theranostics.* 2012;2:437–447.
2. Al-Nahhas A. Nuclear medicine imaging of neuroendocrine tumours. *Clin Med.* 2012;12:377–380.
3. Öberg K. Gallium-68 somatostatin receptor PET/CT: is it time to replace ^{111}indium DTPA octreotide for patients with neuroendocrine tumors? *Endocrine.* 2012;42:3–4.
4. Schreiter NF, Brenner W, Nogami M, et al. Cost comparison of ^{111}In-DTPA-octreotide scintigraphy and ^{68}Ga-DOTATOC PET/CT for staging enteropancreatic neuroendocrine tumours. *Eur J Nucl Med Mol Imaging.* 2012;39:72–82.
5. Kayani I, Bomanji JB, Groves A, et al. Functional imaging of neuroendocrine tumors with combined PET/CT using ^{68}Ga-DOTATATE (DOTA-DPhe1,Tyr3-octreotate) and ^{18}F-FDG. *Cancer.* 2008;112:2447–2455.
6. Ambrosini V, Tomassetti P, Castellucci P, et al. Comparison between ^{68}Ga-DOTA-NOC and ^{18}F-DOPA PET for the detection of gastro-entero-pancreatic and lung neuroendocrine tumours. *Eur J Nucl Med Mol Imaging.* 2008;35:1431–1438.
7. Kroiss A, Putzer D, Uprimny C, et al. Functional imaging in phaeochromocytoma and neuroblastoma with ^{68}Ga-DOTA-Tyr 3-octreotide positron emission tomography and ^{123}I-metaiodobenzylguanidine. *Eur J Nucl Med Mol Imaging.* 2011;38:865–873.
8. Naji M, Zhao C, Welsh SJ, et al. ^{68}Ga-DOTA-TATE PET vs. ^{123}I-MIBG in identifying malignant neural crest tumours. *Mol Imaging Biol.* 2011;13:769–775.
9. Srirajaskanthan R, Kayani I, Quigley AM, Soh J, Caplin ME, Bomanji J. The role of ^{68}Ga-DOTATATE PET in patients with neuroendocrine tumors and negative or equivocal findings on ^{111}In-DTPA-octreotide scintigraphy. *J Nucl Med.* 2010;51:875–882.
10. Putzer D, Gabriel M, Henninger B, et al. Bone metastases in patients with neuroendocrine tumor: ^{68}Ga-DOTA-Tyr3-octreotide PET in comparison to CT and bone scintigraphy. *J Nucl Med.* 2009;50:1214–1221.
11. Frilling A, Sotiropoulos GC, Radtke A, et al. The impact of ^{68}Ga-DOTATOC positron emission tomography/computed tomography on the multimodal management of patients with neuroendocrine tumors. *Ann Surg.* 2010;252:850–856.
12. Versari A, Camellini L, Carlinfante G, et al. Ga-68 DOTATOC PET, endoscopic ultrasonography, and multidetector CT in the diagnosis of duodenopancreatic neuroendocrine tumors: a single-centre retrospective study. *Clin Nucl Med.* 2010;35:321–328.
13. Van Riet J, Rattat D, Verbruggen A, Mortelmans L, Mottaghy FM. Ga-68 DOTATOC PET/CT changed the therapeutic course of a patient with the sudden onset of vision problems. *Clin Nucl Med.* 2009;34:27–28.
14. Froeling V, Elgeti F, Maurer MH, et al. Impact of Ga-68 DOTATOC PET/CT on the diagnosis and treatment of patients with multiple endocrine neoplasia. *Ann Nucl Med.* 2012;26:738–743.
15. Velikyan I. Positron emitting [^{68}Ga]Ga-based imaging agents: chemistry and diversity. *Med Chem.* 2011;7:345–379.
16. Treglia G, Castaldi P, Rindi G, Giordano A, Rufini V. Diagnostic performance of gallium-68 somatostatin receptor PET and PET/CT in patients with thoracic and gastroenteropancreatic neuroendocrine tumours: a meta-analysis. *Endocrine.* 2012;42:80–87.
17. Naji M, Al-Nahhas A. ^{68}Ga-labelled peptides in the management of neuroectodermal tumours. *Eur J Nucl Med Mol Imaging.* 2012;39(suppl 1):S61–S67.
18. Sandström M, Garske-Roman U, Granberg D, et al. Individualized dosimetry of kidney and bone marrow in patients undergoing ^{177}Lu-DOTA-octreotate treatment. *J Nucl Med.* 2013;54:33–41.
19. Beauregard JM, Hofman MS, Kong G, Hicks RJ. The tumour sink effect on the biodistribution of ^{68}Ga-DOTA-octreotate: implications for peptide receptor radionuclide therapy. *Eur J Nucl Med Mol Imaging.* 2012;39:50–56.
20. Maecke HR, Hofmann M, Haberkorn U. ^{68}Ga-labeled peptides in tumor imaging. *J Nucl Med.* 2005;46(suppl 1):172S–178S.
21. Sandström M, Velikyan I, Garske-Román U, et al. Comparative biodistribution and radiation dosimetry of ^{68}Ga-DOTATOC and ^{68}Ga-DOTATATE in patients with neuroendocrine tumors. *J Nucl Med.* 2013;54:1755–1759.
22. Velikyan I, Beyer GJ, Langstrom B. Microwave-supported preparation of ^{68}Ga-bioconjugates with high specific radioactivity. *Bioconjug Chem.* 2004;15:554–560.
23. Velikyan I, Xu H, Nair M, Hall H. Robust labeling and comparative preclinical characterization of DOTA-TOC and DOTA-TATE. *Nucl Med Biol.* 2012;39:628–639.
24. Boellaard R, Oyen WJ, Hoekstra CJ, et al. The Netherlands protocol for standardisation and quantification of FDG whole body PET studies in multi-centre trials. *Eur J Nucl Med Mol Imaging.* 2008;35:2320–2333.
25. Patlak CS, Blasberg RG, Fenstermacher JD. Graphical evaluation of blood-to-brain transfer constants from multiple-time uptake data. *J Cereb Blood Flow Metab.* 1983;3:1–7.
26. Reubi JC, Schär J-C, Waser B, et al. Affinity profiles for human somatostatin receptor subtypes SST1-SST5 of somatostatin radiotracers selected for scintigraphic and radiotherapeutic use. *Eur J Nucl Med.* 2000;27:273–282.
27. Poeppel TD, Binse I, Petersenn S, et al. ^{68}Ga-DOTATOC versus ^{68}Ga-DOTATATE PET/CT in functional imaging of neuroendocrine tumors. *J Nucl Med.* 2011;52:1864–1870.
28. Forrer F, Uusijarvi H, Waldherr C, et al. A comparison of ^{111}In-DOTATOC and ^{111}In-DOTATATE: biodistribution and dosimetry in the same patients with metastatic neuroendocrine tumours. *Eur J Nucl Med Mol Imaging.* 2004;31:1257–1262.
29. Esser JP, Krenning EP, Teunissen JJ, et al. Comparison of [^{177}Lu-DOTA$_0$,Tyr$_3$] octreotate and [^{177}Lu-DOTA$_0$,Tyr$_3$]octreotide: which peptide is preferable for PRRT? *Eur J Nucl Med Mol Imaging.* 2006;33:1346–1351.
30. Velikyan I, Sundin A, Eriksson B, et al. In vivo binding of [^{68}Ga]-DOTATOC to somatostatin receptors in neuroendocrine tumours: impact of peptide mass. *Nucl Med Biol.* 2010;37:265–275.
31. Campana D, Ambrosini V, Pezzilli R, et al. Standardized uptake values of ^{68}Ga-DOTANOC PET: a promising prognostic tool in neuroendocrine tumors. *J Nucl Med.* 2010;51:353–359.
32. Haug AR, Auernhammer CJ, Wangler B, et al. ^{68}Ga-DOTATATE PET/CT for the early prediction of response to somatostatin receptor-mediated radionuclide therapy in patients with well-differentiated neuroendocrine tumors. *J Nucl Med.* 2010;51:1349–1356.
33. Haug AR, Rominger A, Mustafa M, et al. Treatment with octreotide does not reduce tumor uptake of ^{68}Ga-DOTATATE as measured by PET/CT in patients with neuroendocrine tumors. *J Nucl Med.* 2011;52:1679–1683.
34. Gabriel M, Oberauer A, Dobrozemsky G, et al. ^{68}Ga-DOTA-Tyr$_3$-octreotide PET for assessing response to somatostatin-receptor-mediated radionuclide therapy. *J Nucl Med.* 2009;50:1427–1434.